

**Application of rational enzyme engineering in a new route to
Etonorgestrel and Levonorgestrel: Carbonyl reductase bioreduction
of ethyl secodione**

Daniel F.A.R. Dourado^a, Andrew S. Rowan^a, Sergej Maciuk^a, Jenny Spratt^a, Gareth Brown^a, Darren Gray^a, Jill Caswell^a, Alexandra A.T.P. Carvalho^a, Fernando Tur^a, Dražen Pavlović^a, Derek J. Quinn^a, Thomas S. Moody^a and Stefan Mix^{a*}

^a Almac Sciences, Department of Biocatalysis and Isotope Chemistry, UK

Table S1 - Screening of the CREDS from Almac's selectAZyme™ panel. Data of the best enzymes (with minimal formation of ethyl secodiols) are shown. Reaction conditions: 10 mg CRED as lyophilised cell free extract (CFE), 0.5 mg each NAD and NADP, 1 mg glucose dehydrogenase (GDH), 10 mg glucose monohydrate, 2 mg of **4** in 50 µL DMSO, 950 µL 0.1 M potassium phosphate buffer (pH 7) in microcentrifuge tube, shaking overnight at 30 °C).

CRED	% Conversion	% HPLC peak area (products only)					
		(13S,17R)-5	(13R,17S)-5	(13S,17S)-5	(13R,17R)-5	Diol A	Diol B
1	100.00	0.06	98.53	0.03	0.10	1.11	0.16
2	75.04	3.04	0.00	7.40	88.94	0.36	0.27
3	100.00	0.05	99.34	0.07	0.12	0.21	0.21
4	100.00	0.05	99.54	0.03	0.08	0.13	0.17
5	57.53	83.32	0.31	0.93	14.85	0.10	0.49
6	100.00	0.08	0.14	99.16	0.39	0.15	0.09
7 (CRED-BW)	100.00	0.04	98.57	0.12	0.00	1.27	0.00
8	93.86	0.00	0.04	99.57	0.30	0.10	0.00
9	100.00	0.00	99.13	0.06	0.03	0.69	0.09
10	100.00	0.51	0.06	98.44	0.49	0.50	0.00
11	99.81	0.50	0.09	98.68	0.24	0.49	0.00

Table S2 - Screening of the CREDS from Almac's selectAZyme™ panel. Data of the best enzymes at 20 and 50 wt % of CRED loading.

CRED	CRED loading (wt % wrt 4)	% Conv	% HPLC peak area (products only)					
			(13S,17R)-5	(13R,17S)-5	(13S,17S)-5	(13R,17R)-5	Diol A	Diol B
1	50	97.42	0.59	98.87	0.31	0.00	0.23	0.00
3		31.52	1.06	98.67	0.19	0.08	0.00	0.00
4		94.92	0.39	99.53	0.03	0.00	0.04	0.00
CRED-BW		99.67	0.37	99.10	0.03	0.03	0.46	0.00
9		18.76	1.51	97.86	0.38	0.11	0.14	0.00
1	20	45.48	1.42	98.04	0.38	0.00	0.16	0.00
4		55.39	0.63	99.34	0.03	0.00	0.00	0.00
CRED-BW		99.93	0.38	99.48	0.14	0.00	0.00	0.00

Table S3 - CRED-BW amino acid sequence

Code	Organism	Sequence
CRED-BW	Bacillus wiedmannii	MKYTVITGASSGIGYESALAFASRGKNLILVARRQEELDGLKLNEMNPELDVIRRTDLSITENVYKL YESLQTFQIETWINNAGFGNFASIAEQNLNKIETMLHVNIEALTILSSLFVRDYSMVDGTQLINVSSGG G YTIVADAVTYCATKFYVSATFEGLSHELKEQGAKLQAKVLAPAAETETEFAKRSLDIDEFQYNNVVPKFH T AKQMAQFMLDLYSDKVVGIVDGYTYNYELKNPIFNFAVRKTNSSS

Table S4 – CRED-BW Co-Solvent analysis. Screening conditions (0.1 mg (5% w/w) or 0.01 mg (0.5% w/w) CRED-BW (CFE), 0.5 mg NADP, 1 mg glucose dehydrogenase (GDH), 5 mg glucose monohydrate (excess), 2 mg **4** in 50 µL DMSO (5% v/v overall co-solvent), 950 µL 0.1 M potassium phosphate buffer (pH 7)).

Co-solvent	% (v/v) co-solvent	% (w/w) CRED	% Conv
DMSO	5	0.5	91.99
	10	0.5	96.91
	15	0.5	97.78
	30	0.5	70.70
		5	99.92
	50	0.5	7.89
5		24.16	
MTBE	10	0.5	20.33
		5	74.50
Toluene	10	0.5	15.31
		5	21.37
EtOAc	10	0.5	9.52
		5	34.49
Acetone	10	0.5	75.17
		5	99.29
i-PrOAc	10	0.5	4.06
		5	29.88
CPME	10	0.5	2.79
		5	25.12
DIPE	10	0.5	22.51
		5	77.73
MeTHF	10	0.5	7.64
		5	29.44
EtOH	10	0.5	86.57

		5	99.89
IPA	10	0.5	85.35
		5	99.82
1-Octanol	10	0.5	29.68
		5	82.00
2-Octanol	10	0.5	18.86
		5	75.02
2-Ethyl-1-Hexanol	10	0.5	18.18
		5	71.37

Table S5 - CRED-BW temperature analysis. Screening conditions (0.005 mg (0.25% w/w) CRED-BW (CFE), 0.5 mg NADP, 1 mg glucose dehydrogenase (GDH), 5 mg glucose monohydrate (excess), 2 mg **4** in 50 μ L DMSO (5% v/v overall co-solvent), 950 μ L 0.1 M potassium phosphate buffer (pH 7)).

Temperature ($^{\circ}$ C)	% Conv	% HPLC peak area (products only)					
		(13S,17R)-5	(13R,17S)-5	(13S,17S)-5	(13R,17R)-5	Diol A	Diol B
25	25.03	1.27	98.73	0.00	0.00	0.00	0.00
30	45.64	0.72	99.28	0.00	0.00	0.00	0.00
35	64.54	0.56	99.44	0.00	0.00	0.00	0.00
40	38.84	1.15	98.85	0.00	0.00	0.00	0.00

Table S6 - CRED-BW pH analysis. Screening conditions (0.005 mg (0.25% w/w) CRED-BW lyophilised cell free extract (CFE), 0.5 mg NADP, 1 mg glucose dehydrogenase (GDH), 5 mg glucose monohydrate (excess), 2 mg **4** in 50 μ L DMSO (5% v/v overall co-solvent), 950 μ L 0.1 M potassium phosphate buffer (of desired pH), shaken at 35 $^{\circ}$ C overnight).

pH	% Conv
6.2	49.42
6.6	73.67
7.0	79.92
7.4	68.86
7.8	44.39

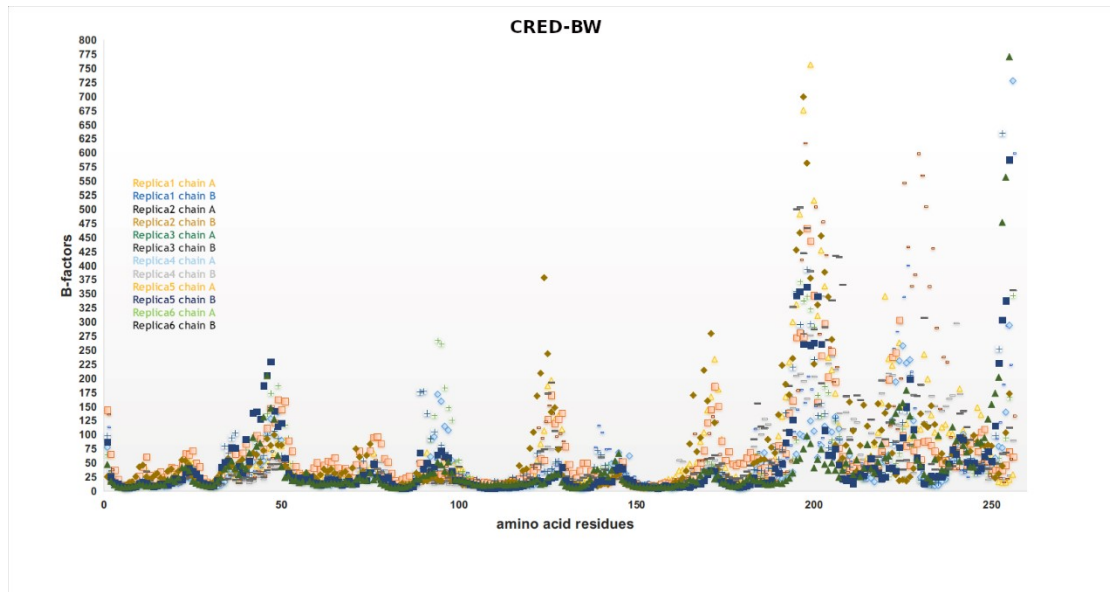


Figure S1: B-factor values for CRED-BW.

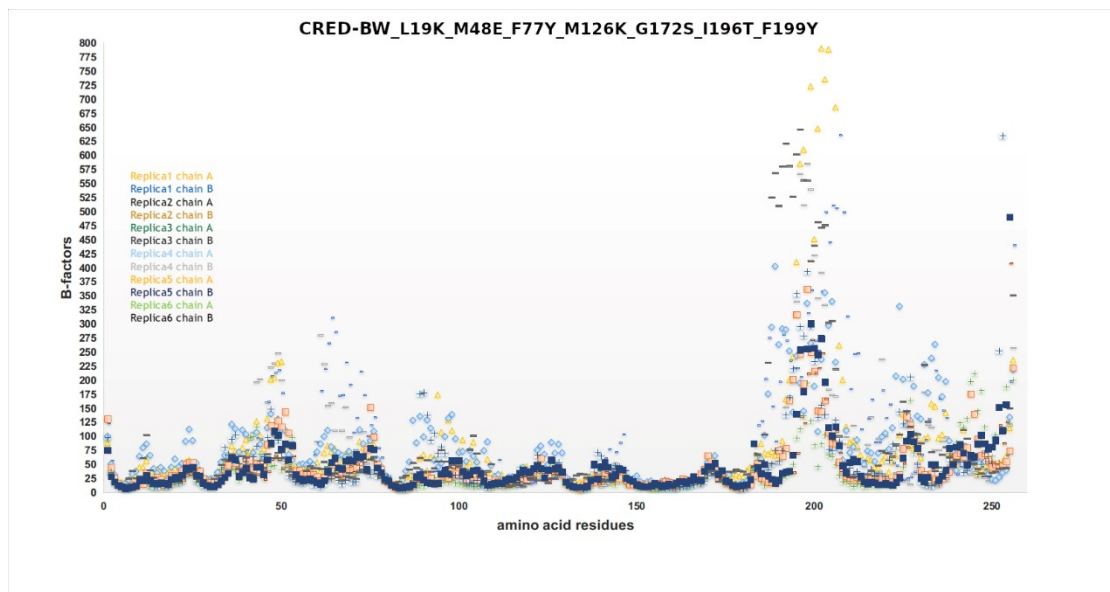


Figure S2: B-factor values for CRED-BW_L19K_M48E_F77Y_M126K_G172S_I196T_F199Y.

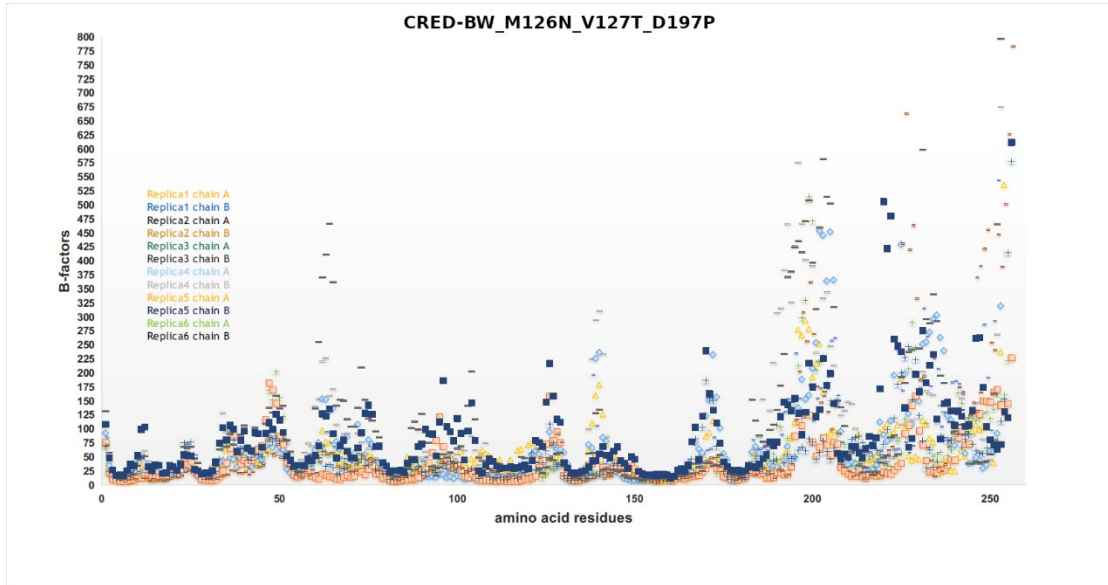


Figure S3: B-factor values for CRED-BW_M126N_V127T_D197P.

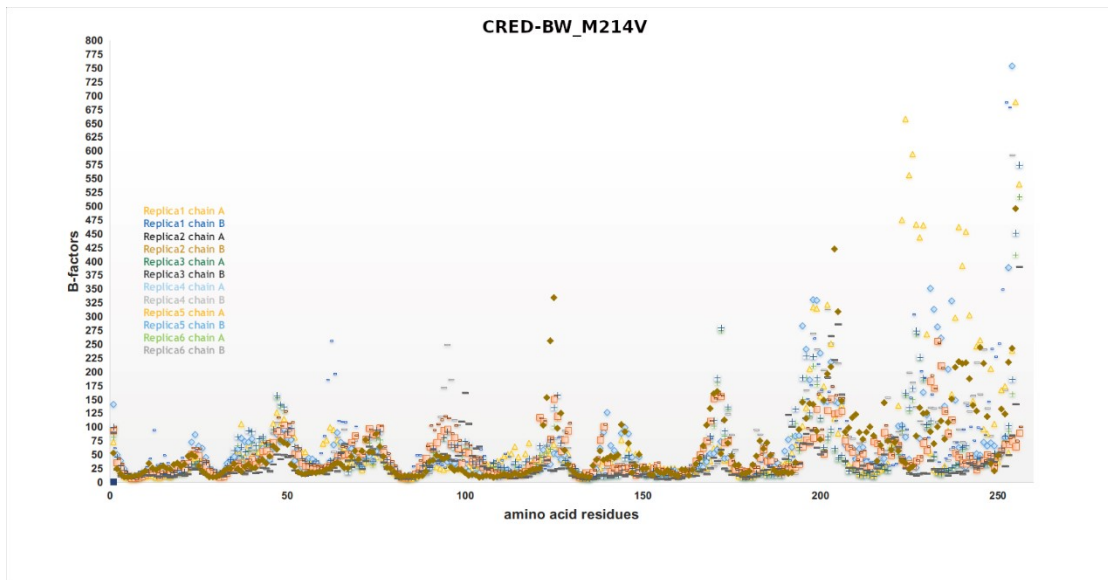


Figure S4 - B-factor values for CRED-BW_M214V

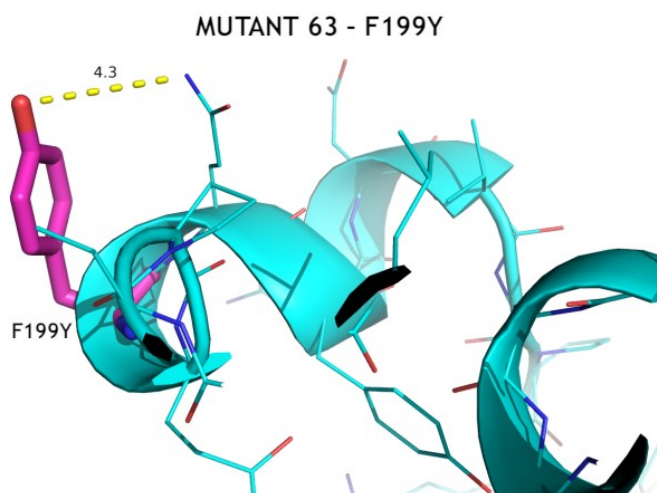
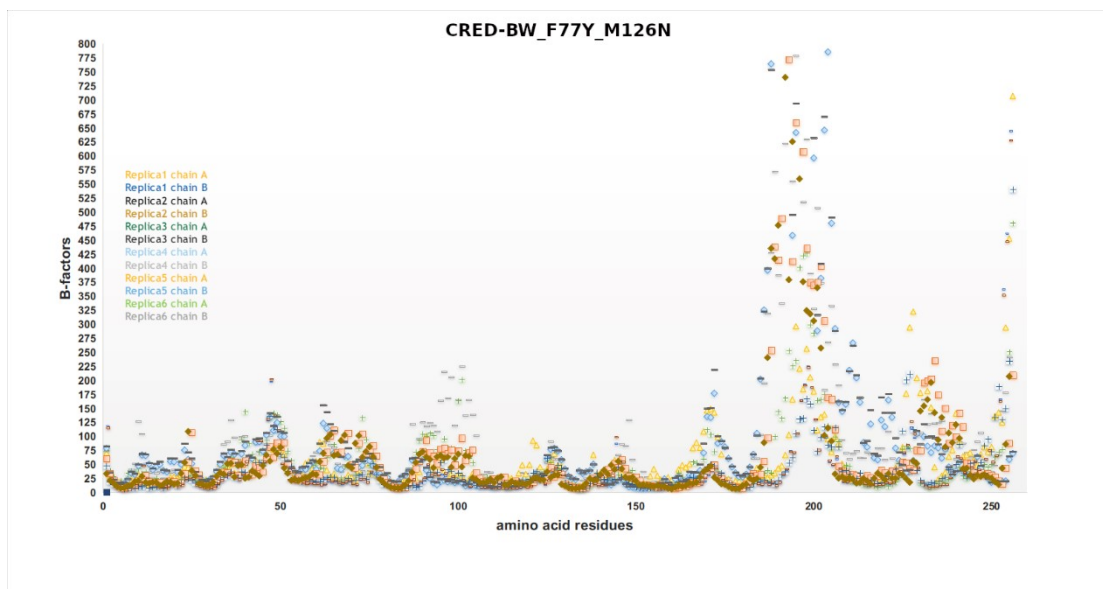


Figure S6 - Mutant 63 - F199Y.

MUTANT 65 - CRED-BW_M126N_V127T_D197P

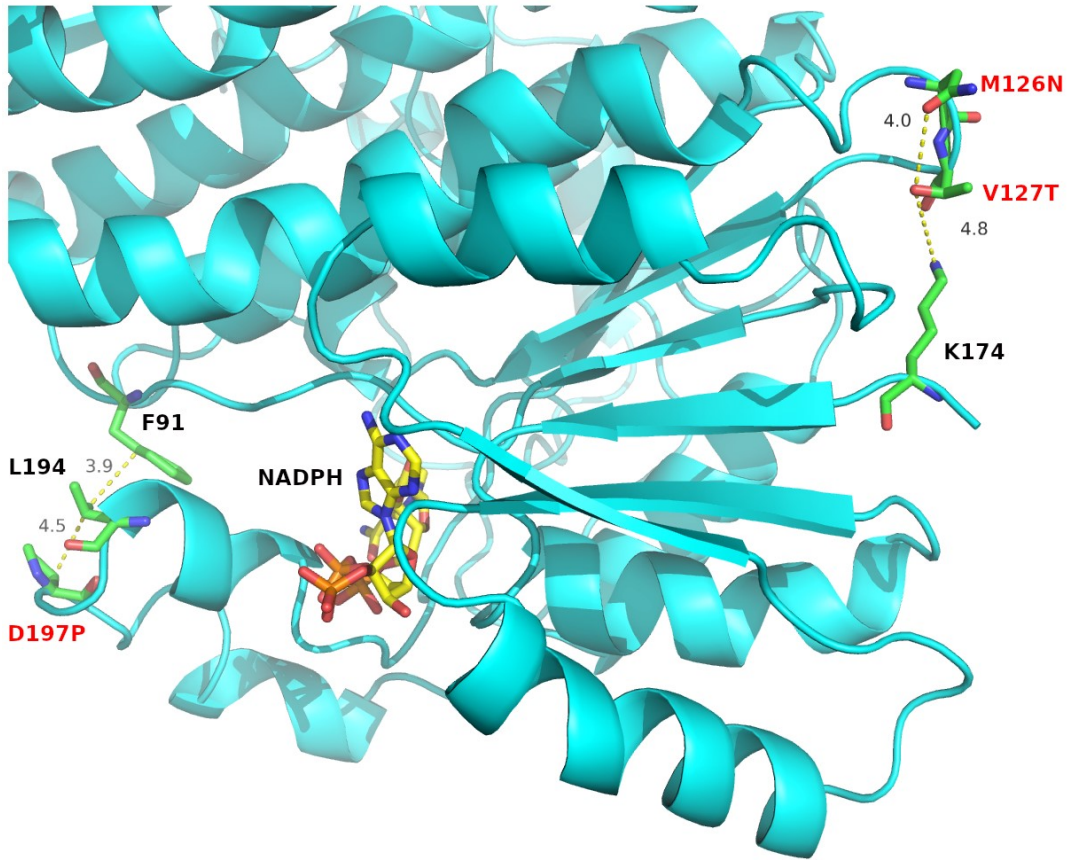


Figure S7 - Mutant 65 - M126N_V127T_D197P

MUTANT 67 - D225R

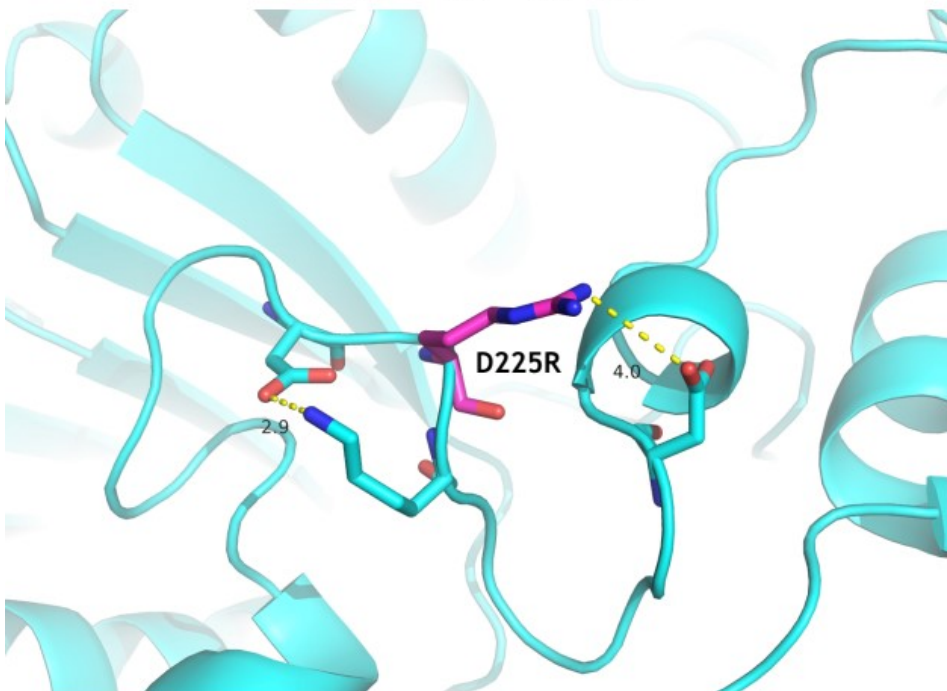


Figure S8 - Mutant 67 - D225R

MUTANT 81 - T59C_V31C

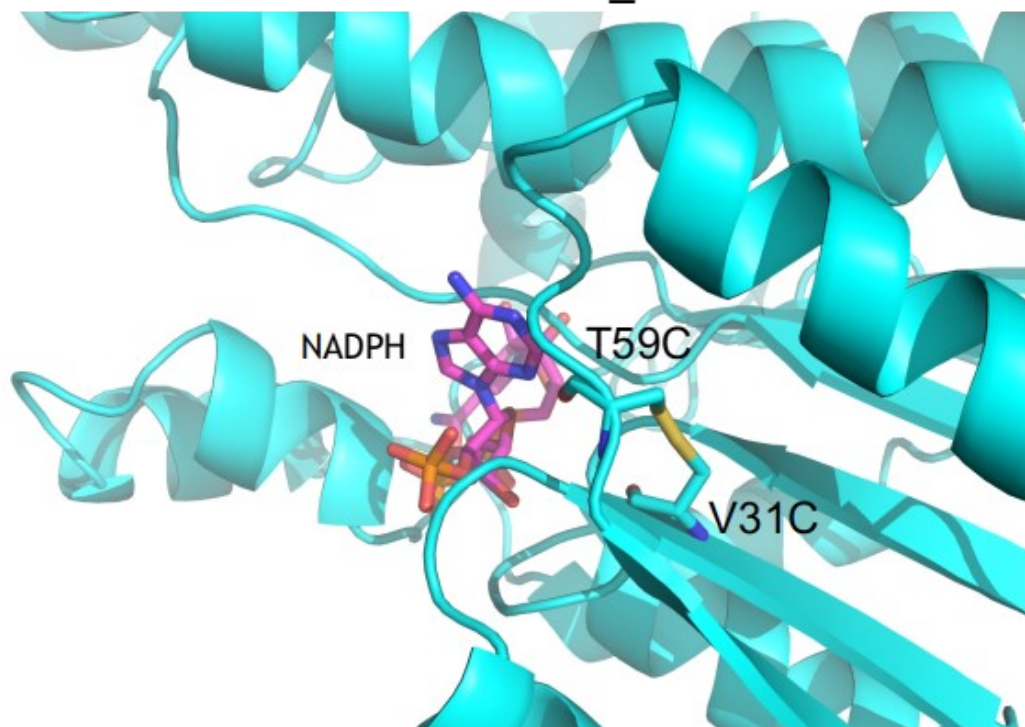


Figure S9 - Mutant 81 - T59C_V31C

Table 7 - CRED-BW mutants

Mutants	Reasoning
MUT1-S17V	Thermal stability
MUT2-L19E	Thermal stability
MUT3-L19K	Thermal stability
MUT4-L19R	Thermal stability
MUT5-L19R_M48E	Thermal stability
MUT6-L19K_M48E	Thermal stability
MUT7-L19E_M48K	Thermal stability
MUT8-L19K_M48K	Thermal stability
MUT9-L19K_M48R	Thermal stability
MUT10-M48E	Thermal stability
MUT11-M48K	Thermal stability
MUT12-M48R	Thermal stability
MUT13-M48I	Thermal stability
MUT14-M48L	Thermal stability
MUT15-T76E	Thermal stability

MUT16-F77Y	Thermal stability
MUT17-M126R	Thermal stability
MUT18-M126K	Thermal stability
MUT19-M126E	Thermal stability
MUT20-M126N	Thermal stability
MUT21-V127S	Thermal stability
MUT22-V127T	Thermal stability
MUT23-G172Q	Thermal stability
MUT24-G172N	Thermal stability
MUT25-G172K	Thermal stability
MUT26-G172S	Thermal stability
MUT27-G172E	Thermal stability
MUT28-G172D	Thermal stability
MUT29-G172P	Thermal stability
MUT30-M126K_G172S	Thermal stability
MUT31-M126K_G172D	Thermal stability
MUT32-M126K_G172K	Thermal stability
MUT33-M126E_G172D	Thermal stability
MUT34-M126N_F77Y	Thermal stability
MUT35-M126K_F77Y	Thermal stability
MUT36-V127T_M126N	Thermal stability
MUT37-V127S_M126N	Thermal stability
MUT38-V127T_M126N_F77Y	Thermal stability
MUT39-I196S	Thermal stability
MUT40-I196T	Thermal stability
MUT41-I196G	Thermal stability
MUT42-I196K	Thermal stability
MUT43-I196E	Thermal stability
MUT44-D197P	Thermal stability
MUT45-D197K	Thermal stability
MUT46-D197S	Thermal stability
MUT47-D197N	Thermal stability
MUT48-D197T	Thermal stability
MUT49-D197E	Thermal stability
MUT50-V135I	Thermal stability
MUT51-E198S	Thermal stability
MUT52-E198T	Thermal stability
MUT53-E198Q	Thermal stability
MUT54-E198N	Thermal stability
MUT55-V125L	Thermal stability
MUT56-E198L	Thermal stability
MUT57-F199S	Thermal stability

MUT58-F199T	Thermal stability
MUT59-F199Q	Thermal stability
MUT60-F199N	Thermal stability
MUT61-F199H	Thermal stability
MUT62-F199G	Thermal stability
MUT63-F199Y	Thermal stability
MUT64-I196T_F199Y	Thermal stability
MUT65-V127T_M126N_D197P	Thermal stability
MUT66-D225K	Thermal stability
MUT67-D225R	Thermal stability
MUT68-L219Y	Thermal stability
MUT69-L219T	Thermal stability
MUT70-L219D	Thermal stability
MUT71-M105I	Stability/Methionine oxidation prevention
MUT72-M105L	Stability/Methionine oxidation prevention
MUT73-M105E	Stability/Methionine oxidation prevention
MUT74-M105Q	Stability/Methionine oxidation prevention
MUT75-M214V	Stability/Methionine oxidation prevention
MUT76-M214I	Stability/Methionine oxidation prevention
MUT77-M214T MUT778-M218A	Stability/Methionine oxidation prevention
MUT79-M218I	Stability/Methionine oxidation prevention
MUT80-M218S	Stability/Methionine oxidation prevention
MUT81- V31C_T59C	Stability / SSbond
MUT82- L116C_W82C	Stability / SSbond
MUT83- V31C_T59C_L116C-W82C	Stability / SSbond
Mut84- E37K	Stability in organic solvent
Mut85-K44E	Stability in organic solvent
Mut86-E80K	Stability in organic solvent
Mut87-D128K	Stability in organic solvent
Mut88-K169E	Stability in organic solvent
Mut89-E188K	Stability in organic solvent
Mut90-K191E	Stability in organic solvent
Mut91-K191D	Stability in organic solvent
Mut92-R192D	Stability in organic solvent
Mut93-R192E	Stability in organic solvent